FLUIDS WITH INTERNAL DEGREES OF FREEDOM

F. LADO
Department of Physics
North Carolina State University
Raleigh, NC, 27695-8202, USA

1. Introduction

The essential core of the modern integral equation approach to liquid state theory was arrived at nearly simultaneously in 1960 by a remarkable number of authors working independently [1]. They found that the density expansion of the pair distribution function $g(r)$ of a simple fluid with interatomic potential $\phi(r)$ could be grouped into infinite subsets of diagrams such that

$$g(r)e^{\beta\phi(r)} = 1 + S(r) + P(r) + B(r), \tag{1}$$

where, in the pictorial electrical language of M. S. Green [2], the diagrams of the *series* set $S(r)$ resemble series circuits and those of the *parallel* set $P(r)$ resemble parallel circuits; the remaining *bridge* set $B(r)$ begins with a diagram that looks like a Wheatstone bridge. Further, the diagrams of $P(r)$ could be summed in direct space to give $P(r) = g(r)\exp(\beta\phi(r)) - 1 - \ln[g(r)\exp(\beta\phi(r))]$, while those of $S(r)$ could be summed in Fourier space to yield $\tilde{S}(k) = \tilde{c}^2(k)/[1-\rho\tilde{c}(k)]$, which is the Ornstein-Zernike (OZ) equation in Fourier transform representation. Here, $c(r) = h(r) - S(r)$ is the sum of non-nodal graphs, or *direct correlation function*, while $h(r) = g(r) - 1$ is the *total correlation function*. In brief, the upshot of these analyses was that $g(r)$, the key to all fluid properties, could be obtained by the iteration of a simple, four-step recipe for the unknown $S(r)$, now more often denoted $\gamma(r)$ and called the *indirect correlation function*:

1. *Closure:* $\gamma(r) \to c(r)$.

$$c(r) = \exp[-\beta\phi(r) + \gamma(r) + B(r)] - 1 - \gamma(r) \tag{2}$$

2. *Transform:* $c(r) \to \tilde{c}(k)$.

$$\tilde{c}(k) = \frac{4\pi}{k}\int_0^\infty dr\, rc(r)\sin(kr) \tag{3}$$

3. *OZ equation:* $\tilde{c}(k) \to \tilde{\gamma}(k)$.

$$\tilde{\gamma}(k) = \rho\tilde{c}^2(k)/[1 - \rho\tilde{c}(k)] \tag{4}$$

4. *Inverse transform:* $\tilde{\gamma}(k) \to \gamma(r)$.

$$\gamma(r) = \frac{1}{2\pi^2 r}\int_0^\infty dk\, k\tilde{\gamma}(k)\sin(kr) \tag{5}$$

Upon convergence, meaning the output $\gamma(r)$ from (5) matches the input $\gamma(r)$ in (2), the pair distribution function is found as $g(r) = \exp[-\beta\phi(r) + \gamma(r) + B(r)]$. In these equations, ρ is the number density and $\beta = 1/k_BT$.

This recipe of course requires knowing $B(r)$. But the bridge function diagrams could not be summed and the original authors all hopefully proposed $B(r) \approx 0$ as a first approximation. The result, known as the hypernetted chain (HNC) equation, in fact was predated by the Percus-Yevick equation, obtained in a completely different fashion [3] but equivalent to $B(r) \approx -P(r)$. These familiar closures have since been supplemented with numerous other approximations for $B(r)$ [1] but remain still popular today.

Equations (2)-(5) apply to "simple" fluids in three dimensions with spherically symmetric potentials $\phi(r)$. They can be generalized for "molecular" fluids [4], with potentials $\phi(\mathbf{r}, \omega_1, \omega_2)$ that depend on orientational degrees of freedom ω in addition to the interparticle separation $\mathbf{r}$. The generalization is based on orthogonal expansions in the angular variables. In the present work, I am concerned with a further generalization to fluids whose molecules have *internal* degrees of freedom, such as size σ with distribution $f(\sigma)$ or polarization $\mathbf{p}$ with distribution $f_0(p)$ for an isolated molecule. In the latter case, the dipole-dipole interactions will rearrange the distribution $f_0(p)$ in dense fluids into a new shape $f(p)$ that is an additional unknown. The new generalization will similarly be based on expansions in the additional variables, σ, $\mathbf{p}$, *etc.*, but now the basis functions will be explicitly constructed to be orthogonal with weight function $f(\sigma)$, $f(p)$, *etc.*

2. Polydisperse colloidal fluids

Colloidal particles are stable conglomerates of atoms whose length scale is on the boundary between the microscopic and macroscopic worlds. The description of the structure of these liquid-like suspensions using the tools of simple atomic liquids is complicated primarily by the fact that the particles of any given suspension display a continuous distribution of sizes; *i.e.*, they are inherently *polydisperse*.

Let $f(\sigma)$ be the distribution of particle diameters σ in a homogeneous assembly of N polydisperse colloidal particles contained in volume V at

temperature T. The density of particles at point $\mathbf{r}$ with diameter σ is then

$$\rho^{(1)}(\mathbf{r},\sigma) =< \sum_{i=1}^{N} \delta(\mathbf{r}-\mathbf{r}_i)\delta(\sigma-\sigma_i) >= \rho f(\sigma), \tag{6}$$

where $\rho = N/V$, while the two-body density is

$$\begin{aligned} \rho^{(2)}(\mathbf{r},\sigma,\mathbf{r}',\sigma') &= < \sum_{i\neq j} \delta(\mathbf{r}-\mathbf{r}_i)\delta(\sigma-\sigma_i)\delta(\mathbf{r}'-\mathbf{r}_j)\delta(\sigma'-\sigma_j) > \\ &= \rho^2 f(\sigma) f(\sigma') g(|\mathbf{r}-\mathbf{r}'|,\sigma,\sigma'), \end{aligned} \tag{7}$$

which defines the pair distribution function $g(r,\sigma,\sigma')$. In these expressions, $\mathbf{r}_i$ is the location of particle i and σ_i its diameter; the brackets denote a canonical ensemble average.

The generalized OZ equation between $\gamma(r,\sigma_1,\sigma_2)$ and $c(r,\sigma_1,\sigma_2)$ can again be deconvoluted using Fourier transforms and now yields

$$\tilde{\gamma}(k,\sigma_1,\sigma_2) = \rho \int_0^\infty d\sigma_3 f(\sigma_3)[\tilde{c}(k,\sigma_1,\sigma_3) + \tilde{\gamma}(k,\sigma_1,\sigma_3)]\tilde{c}(k,\sigma_3,\sigma_2), \tag{8}$$

with one remaining integral. The final integration in Eq. (8) can also be eliminated and the evaluation of the OZ equation reduced to algebra by now expanding all σ-dependent functions in orthogonal polynomials $p_j(\sigma)$, $j = 0, 1, 2, \ldots$, defined such that

$$\int_0^\infty d\sigma\, f(\sigma) p_i(\sigma) p_j(\sigma) = \delta_{ij}, \tag{9}$$

where δ_{ij} is the Kronecker delta. Then with

$$\tilde{\gamma}(k,\sigma_1,\sigma_2) = \sum_{i,j=0}^{\infty} \tilde{\gamma}_{ij}(k) p_i(\sigma_1) p_j(\sigma_2) \tag{10}$$

and a similar expansion of $\tilde{c}(k,\sigma_1,\sigma_2)$, Eq. (8) becomes

$$\tilde{\gamma}_{ij}(k) = \rho \sum_l [\tilde{c}_{il}(k) + \tilde{\gamma}_{il}(k)]\tilde{c}_{lj}(k), \tag{11}$$

which are now matrix equations. Orthonormality allows the easy inversion of Eq. (10); similar expansions and inversions hold for functions in r space. The inversion of $c(r,\sigma_1,\sigma_2)$, for example, is shown below in Eq. (14). The four-step recipe now becomes

1. *Closure:* $\gamma_{ij}(r) \to c_{ij}(r)$. Form

$$\gamma(r,\sigma_1,\sigma_2) = \sum_{i,j} \gamma_{ij}(r) p_i(\sigma_1) p_j(\sigma_2), \tag{12}$$

$$c(r,\sigma_1,\sigma_2) = \exp[-\beta\phi(r,\sigma_1,\sigma_2) + \gamma(r,\sigma_1,\sigma_2) + B(r,\sigma_1,\sigma_2)] - 1 - \gamma(r,\sigma_1,\sigma_2), \tag{13}$$

and numerically evaluate the coefficients

$$c_{ij}(r) = \int d\sigma_1 d\sigma_2 f(\sigma_1) f(\sigma_2) c(r,\sigma_1,\sigma_2) p_i(\sigma_1) p_j(\sigma_2) \tag{14}$$

using n-point Gaussian quadrature based on the zeroes of $p_n(\sigma)$.

2. *Transforms:* $c_{ij}(r) \to \tilde{c}_{ij}(k)$, as in Eq. (3).
3. *OZ equation:* $\tilde{c}_{ij}(k) \to \tilde{\gamma}_{ij}(k)$.

$$\tilde{\Gamma}(k) = \rho\tilde{C}(k)\tilde{C}(k)[I - \rho\tilde{C}(k)]^{-1} \tag{15}$$

Here $\tilde{\Gamma}(k)$ and $\tilde{C}(k)$ are symmetric matrices with elements $\tilde{\gamma}_{ij}(k)$ and $\tilde{c}_{ij}(k)$, respectively, and I is the unit matrix.

4. *Inverse transforms:* $\tilde{\gamma}_{ij}(k) \to \gamma_{ij}(r)$, as in Eq. (5).

With a converged solution in hand, the thermodynamic properties of the colloidal suspension, such as internal energy U, pressure p, and isothermal compressibility K_T, are readily obtained by quadratures. Further, the Helmholtz free energy A can also be obtained [5] from the coefficients of the pair functions in, for example, HNC approximation.

Such calculations have been carried out [5] for charge-stabilized, polydisperse colloidal suspensions whose particle diameters σ are distributed about a mean diameter $\bar{\sigma}$ according to the Schulz distribution,

$$f(\sigma) = \left(\frac{\alpha+1}{\bar{\sigma}}\right)^{\alpha+1} \frac{\sigma^\alpha e^{-(\alpha+1)\sigma/\bar{\sigma}}}{\Gamma(\alpha+1)}, \tag{16}$$

where $\Gamma(z)$ is the gamma function. The relative standard deviation of this distribution is $s_\sigma \equiv (<\sigma^2> - <\sigma>^2)^{1/2}/<\sigma> = (\alpha+1)^{-1/2}$, which is used to characterize the suspensions and define the parameter α. The orthonormal polynomials for the Schulz distribution are

$$p_j(\sigma) = \left[\frac{j!\Gamma(\alpha+1)}{\Gamma(j+\alpha+1)}\right]^{1/2} L_j^\alpha\left((\alpha+1)\frac{\sigma}{\bar{\sigma}}\right), \tag{17}$$

where the $L_j^\alpha(t)$ are the associated Laguerre polynomials.

The charged mesospheres are assumed to have a constant surface charge density, so that their charge polydispersity is mapped onto the size polydispersity according to $Z(\sigma) = Z_{\bar{\sigma}}(\sigma/\bar{\sigma})^2$, where $Z_{\bar{\sigma}}$ is the charge on a particle

TABLE 1. Thermodynamics of a polydisperse colloidal suspension with screened Coulomb potential and Schulz distribution of relative standard deviation s_σ; MC data are from D'Aguanno and Klein [6].

	s_σ	$\beta U/N$	$\beta p/\rho$	$\rho k_B T K_T$	$\beta A/N$
MC		28.00	48.50		
RY	0	28.30	48.78	0.00851	
HNC		28.71	49.20	0.00999	31.91
MC		27.66	48.14		
RY	0.1	27.94	48.45	0.00854	
HNC		28.35	48.87	0.01005	31.55
MC		26.64	47.16		
RY	0.2	26.89	47.48	0.00863	
HNC		27.31	47.90	0.01025	30.49
MC		24.97	45.50		
RY	0.3	25.24	45.86	0.00879	
HNC		25.67	46.30	0.01059	28.83

of mean diameter $\bar{\sigma}$, and to interact, beyond hard sphere contact, through a screened Coulomb potential,

$$\beta\phi(r,\sigma_1,\sigma_2) = \begin{cases} \infty, & \text{if } r < \sigma_{12} \\ A(\sigma_1)A(\sigma_2)\exp(-\kappa r)/r, & \text{if } r > \sigma_{12} \end{cases} , \qquad (18)$$

where $\sigma_{12} = (\sigma_1 + \sigma_2)/2$ and $A(\sigma) = Z(\sigma)L_B^{1/2}\exp(\kappa\sigma/2)/(1+\kappa\sigma/2)$. Here, $L_B = e^2/4\pi\epsilon_0\epsilon k_B T$ is the Bjerrum length and $\kappa = (4\pi L_B \rho \bar{Z})^{1/2}$ is the inverse Debye-Hückel screening length, with $\bar{Z} = Z_{\bar{\sigma}}(1+s_\sigma^2)$.

This is the same model studied by D'Aguanno and Klein [6], who judiciously converted the polydisperse system to a finite mixture of discrete diameters. To illustrate the polynomial expansion method, I have recalculated their results for the state with $\bar{\sigma} = 250$ Å, $Z_{\bar{\sigma}} = 200$, and $L_B = 7.01$ Å, at the reduced density $\rho\bar{\sigma}^3 = 0.005$, using the HNC and Rogers-Young (RY) [7] closures,

The computed thermodynamic values are shown in Table 1 for three Schulz distributions of increasing width, $s_\sigma = 0.1$, 0.2, and 0.3, as well as the monodisperse case, $s_\sigma = 0$, for reference. The present integral equation results are in good agreement with those found earlier [6] using the "mixture" method.

Pair functions of interest can be expressed directly in terms of the computed coefficients $g_{ij}(r)$. In particular, the number-number pair distribution function $g_{NN}(r)$ [6] is precisely $g_{00}(r)$. Further, local fluctuations in density

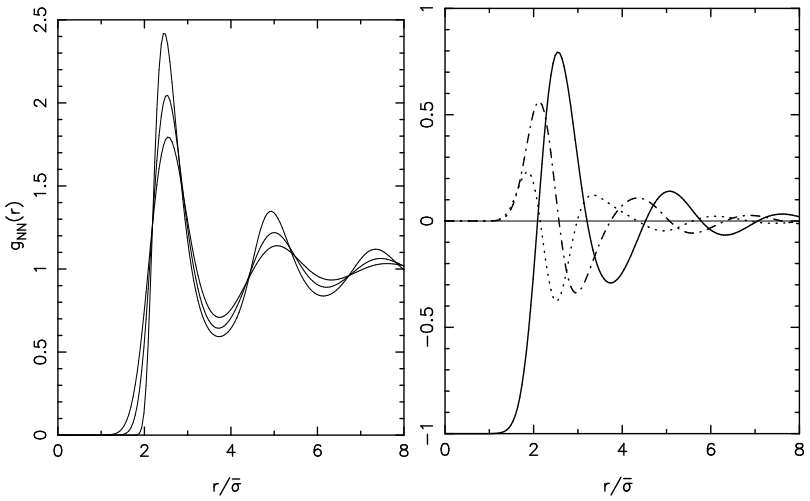

Figure 1. Pair distribution function coefficients for a polydisperse colloidal *monolayer* with screened Coulomb potential at density $\rho\bar{\sigma}^2 = 0.15$, from the RY equation. (a) *Left figure.* $g_{NN}(r) = g_{00}(r)$ for size dispersion of the spheres, in descending order of the first peak, of $s_\sigma = 0$, 0.2, and 0.3. (b) *Right figure.* $g_{00}(r) - 1$ (solid line), $g_{10}(r)$ (dash-dot line), and $g_{11}(r)$ (dotted line) for size dispersion $s_\sigma = 0.3$.

and size may be expressed in normalized form as

$$\delta\rho_0(\mathbf{r}) = \frac{1}{\rho}\left(\sum_{j=1}^{N}\delta(\mathbf{r}-\mathbf{r}_j) - \rho\right), \tag{19}$$

$$\delta\rho_1(\mathbf{r}) = \frac{1}{\bar{\sigma}\rho s_\sigma}\left(\sum_{j=1}^{N}\sigma_j\delta(\mathbf{r}-\mathbf{r}_j) - \bar{\sigma}\rho\right). \tag{20}$$

Their spatial correlations are then given by

$$< \delta\rho_0(\mathbf{r})\delta\rho_0(\mathbf{0}) > = \frac{\delta(\mathbf{r})}{\rho} + [g_{00}(r) - 1], \tag{21}$$

$$< \delta\rho_1(\mathbf{r})\delta\rho_0(\mathbf{0}) > = -g_{10}(r), \tag{22}$$

$$< \delta\rho_1(\mathbf{r})\delta\rho_1(\mathbf{0}) > = \frac{\delta(\mathbf{r})}{\rho} + g_{11}(r). \tag{23}$$

Rather than show these correlation functions for the three-dimensional calculation described above, I display instead the results for a similar quasi-two-dimensional polydisperse colloidal *monolayer* [8]. [The only change needed in the calculation algorithm for the 2D version is the replacement of the Fourier transforms, with kernel $\sin(kr)$, by Hankel transforms, with kernel $J_0(kr)$, in Steps 2 and 4, where $J_0(x)$ is the Bessel function of order

zero.] The effect of growing polydispersity on the number-number distribution function $g_{NN}(r)$ is seen in Fig. 1(a) for $\rho\bar{\sigma}^2 = 0.15$. The general pattern of decreasing structure with increasing dispersion reproduces the behavior of polydisperse colloids in three dimensions [6]. The functions $g_{00}(r) - 1$, $g_{10}(r)$, and $g_{11}(r)$ for correlations of density-density, size-density, and size-size fluctuations, respectively, Eqs. (21)-(23), are shown in Fig. 1(b) for density $\rho\bar{\sigma}^2 = 0.15$ and dispersion $s_\sigma = 0.3$. We see, for example, that at the first peak of $g_{00}(r)$, which occurs at $r = 2.54\bar{\sigma}$, the size-size fluctuations are *negatively* correlated, while the cross correlation of size and density fluctuations passes through zero. This means that large spheres (large charges) are generally surrounded by small spheres (small charges) and vice versa.

These results are obtained for the same size-distribution, Eq. (16), and potential, Eq. (18), as the three-dimensional model. The potential parameters used are the experimental values of Crocker and Grier [9]: $\bar{\sigma} = 650$ nm, $L_B = 0.715$ nm, $\kappa\bar{\sigma} = 4.0$, and $Z_{\bar{\sigma}} = 1990$. Under these conditions, electrostatic repulsion keeps the hard spheres from touching, so that only charge polydispersity is relevant in practice.

3. Polarizable nonpolar fluids

Molecules lacking a permanent dipole moment will nonetheless display instantaneous moments $\mathbf{p}$ that fluctuate randomly within some overall constraints and so will interact through dipole-dipole forces with other such molecules. I will follow Høye and Stell [10] and Pratt [11] in assuming an intrinsic thermal distribution of Gaussian form,

$$f_0(p) = \frac{1}{(2\pi\alpha_0/\beta)^{3/2}} \exp\left(-\frac{\beta p^2}{2\alpha_0}\right), \tag{24}$$

for the spontaneous dipole moment $\mathbf{p}$ of an isolated molecule, where α_0 is its polarizability. These authors have independently solved the mean spherical approximation (MSA) for this model (with inclusion of a permanent dipole in the case of the Høye-Stell work) and find that the fluctuating dipole distribution $f(p)$ in the dense liquid remains Gaussian, an inherent restriction of the MSA, with a larger polarizability α. The present approach [12] removes any such prior restriction.

We consider then a system of N molecules, each with intrinsic polarizability α_0 and fluctuating polarity but no permanent dipole moment, interacting pairwise through through a Lennard-Jones (LJ) potential,

$$u_0(r) = 4\epsilon[(\sigma/r)^{12} - (\sigma/r)^6], \tag{25}$$

and the usual dipole-dipole potential,

$$u_{dd}(\mathbf{r}, \mathbf{p}_1, \mathbf{p}_2) = -\frac{1}{r^3}[3(\hat{\mathbf{r}} \cdot \mathbf{p}_1)(\hat{\mathbf{r}} \cdot \mathbf{p}_2) - \mathbf{p}_1 \cdot \mathbf{p}_2]. \tag{26}$$

The one-body and two-body densities are defined as in Eqs. (6) and (7) with $\mathbf{p}$ replacing σ, so we get $\rho^{(1)}(\mathbf{r},\mathbf{p}) = \rho f(p)$ and $\rho^{(2)}(\mathbf{r},\mathbf{p},\mathbf{r}',\mathbf{p}') = \rho^2 f(p) f(p') g(\mathbf{r}-\mathbf{r}',\mathbf{p},\mathbf{p}')$, where now both f and g are to be determined. The two distribution functions are of course coupled by the intermolecular potential u_{dd}. A direct expression of this coupling is obtained by differentiating $f(p)$ to yield

$$\frac{d}{dp}\ln\left[\frac{f(p)}{f_0(p)}\right] = -\rho\int d\mathbf{r}d\mathbf{p}'\, f(p')g(\mathbf{r},\mathbf{p},\mathbf{p}')\beta u_{dd}(\mathbf{r},\hat{\mathbf{p}},\mathbf{p}'), \tag{27}$$

the first member of a Kirkwood-Born-Green-Yvon hierarchy. The plan now will be to calculate $g(\mathbf{r},\mathbf{p},\mathbf{p}')$ for a given $f(p)$ [starting with $f_0(p)$] using a procedure like that for polydisperse systems and then return to Eq. (27) to update $f(p)$. This will begin a new round for an updated g, and so the process continues until both f and g are self-consistently determined.

The conventional first step in solving molecular equations is to explicitly break out the angular dependence of all functions in the form of expansions in spherical harmonics [4]; *e.g.*,

$$\begin{aligned}\gamma(\mathbf{r},\mathbf{p}_1,\mathbf{p}_2) &= \gamma(r,p_1,p_2,\omega_1,\omega_2)\\ &= 4\pi\sum_{l_1,l_2,m}\gamma_{l_1l_2m}(r,p_1,p_2)Y_{l_1m}(\omega_1)Y_{l_2\bar{m}}(\omega_2),\end{aligned} \tag{28}$$

where $\bar{m} = -m$. In this and similar expressions, the vector $\mathbf{r}$ has been implicitly chosen as the z direction in the specification of the Euler angles $\omega = (\theta,\phi)$. What makes this expansion particularly useful is of course the orthogonality of the spherical harmonics, so that the coefficients of the expansion are immediately obtainable by quadratures.

We now similarly break out the fluctuating-dipole dependence in the form of expansions in polynomials of p,

$$\gamma_{l_1l_2m}(r,p_1,p_2) = \sum_{n_1,n_2}\gamma^{n_1n_2}_{l_1l_2m}(r)Q_{n_1l_1}(p_1)Q_{n_2l_2}(p_2), \tag{29}$$

which are constructed to be orthogonal with weight function $f(p)$,

$$4\pi\int_0^\infty dp\, p^2 f(p)Q_{nl}(p)Q_{n'l}(p) = \delta_{nn'}, \tag{30}$$

so that coefficients of the expansion are again obtainable by quadratures.

Since the distribution function $f(p)$ will evolve during the course of an iterative solution, the associated polynomials $Q_{nl}(p)$ will also change. In principle, for a general $f(p)$ one may have to determine the $Q_{nl}(p)$ by elementary methods, such as Gram-Schmidt orthogonalization [13], starting

TABLE 2. Computed thermodynamic and electrostatic properties of a polarizable nonpolar Lennard-Jones liquid for states characterized by ρ, T, and α_0 values; molecular dynamics values of the dielectric constant ε are from Pollock and Alder [16].

$\rho\sigma^3$	k_BT/ϵ	α_0/σ^3	$\beta U/N$	$\beta p/\rho$	ξ_2	ξ_4	α/σ^3	ε	
								RHNC	MD
0.84	0.70	0.02	-8.709	-0.213	-0.007	0.000	0.0201	1.227	1.23
0.84	0.72	0.05	-8.470	-0.023	-0.041	0.000	0.0514	1.646	1.64
0.20	2.01	0.10	-0.689	0.808	-0.037	0.001	0.1025	1.280	1.27
0.70	1.97	0.10	-2.332	2.028	-0.144	0.001	0.1096	2.284	2.24
0.84	0.67	0.10	-9.304	-0.686	-0.167	0.001	0.1112	2.688	2.64
0.84	0.80	0.14	-7.825	0.486	-0.362	0.003	0.1738	4.150	3.94

from $Q_{00}(p) = 1$. At least initially, however, the distribution $f(p)$ in the present calculation will be Gaussian and the needed polynomials are immediately found in the form of the eigenfunctions of the quantum-mechanical harmonic oscillator in three dimensions using spherical coordinates. For a Gaussian distribution of variance α/β, they are [14]

$$Q_{nl}(p) = \left[\frac{\Gamma\left(\frac{1}{2}(n-l)+1\right)\Gamma\left(\frac{3}{2}\right)}{\Gamma\left(\frac{1}{2}(n+l)+\frac{3}{2}\right)}\right]^{1/2}\left(\frac{\beta p^2}{2\alpha}\right)^{l/2} L^{l+\frac{1}{2}}_{\frac{1}{2}(n-l)}\left(\frac{\beta p^2}{2\alpha}\right). \quad (31)$$

For the cases studied in Ref. [12], it turns out that in fact the computed deviations of $f(p)$ from a Gaussian are very small, permitting retention of these polynomials (with changing α) for the entire calculation.

With the internal degrees of freedom included in the expansion bases, the solution of the (OZ+closure) equations for a polarizable fluid follows along a path already taken for purely molecular fluids [15] and polydisperse colloids [5]. Thus, upon introducing the full expansions for $\tilde{\gamma}$ and $\tilde{c}$ and exploiting the orthonormality of the basis functions, one finds that the OZ equation again goes over into a set of matrix equations for the respective coefficients,

$$\tilde{\gamma}^{n_1n_2}_{l_1l_2m}(k) = (-1)^m\rho\sum_{n_3,l_3}\left[\tilde{\gamma}^{n_1n_3}_{l_1l_3m}(k) + \tilde{c}^{n_1n_3}_{l_1l_3m}(k)\right]\tilde{c}^{n_3n_2}_{l_3l_2m}(k), \quad (32)$$

which has the solution, in matrix notation,

$$\tilde{\Gamma}_m(k) = (-1)^m\rho\tilde{C}_m(k)\tilde{C}_m(k)\left[I - (-1)^m\rho\tilde{C}_m(k)\right]^{-1}. \quad (33)$$

Here $\tilde{\Gamma}_m(k)$ and $\tilde{C}_m(k)$ are symmetric matrices with elements $\tilde{\gamma}^{n_1n_2}_{l_1l_2m}(k)$ and $\tilde{c}^{n_1n_2}_{l_1l_2m}(k)$, respectively, $n, l \geq m$, and I is the unit matrix.

The simplification these expansions effect is immediately reflected in the evaluation of Eq. (27) for $f(p)$, which can now be integrated to give the explicit solution [12]

$$\ln\left[\frac{f(p)}{f_0(p)}\right] = \sum_{n=2,4,6,\ldots}\left(\frac{4}{3n}\right)^{1/2}\xi_n Q_{n0}(p) = \sum_{j=1}^{\infty}\left(\frac{2}{3j}\right)^{1/2}\xi_{2j}\hat{L}_j^{1/2}\left(\frac{\beta p^2}{2\alpha}\right), \tag{34}$$

$$\xi_n = \frac{1}{2}\rho\int d\mathbf{r}\sum_{m=-1,0,1} g_{11m}^{n-1,1}(r)\beta u_{11\bar{m}}^{11}(r). \tag{35}$$

Here $\hat{L}_j^{1/2}(t)$ is the associated Laguerre polynomial renormalized to unity.

The computed coefficients of g will now yield not only the usual thermodynamic properties as before but also the electrostatic properties of the model; in particular, the dielectric constant is given by [12]

$$\varepsilon = \frac{1-\rho\tilde{h}_{111}^{11}(0)}{1+\rho\tilde{h}_{110}^{11}(0)}. \tag{36}$$

The calculated properties of a system of nonpolar polarizable Lennard-Jones molecules are summarized in Table 2 for six states for which molecular dynamics (MD) data of Pollock and Alder [16] are available. The specific closure used is the optimized reference-HNC (RHNC) approximation [17, 18, 19], with the bridge function B represented by just a spherically symmetric hard-sphere term, $B(\mathbf{r},\mathbf{p}_1,\mathbf{p}_2) \approx B_{\rm HS}(r;\sigma_{\rm HS})$. A better approximation would include at least the same coefficients of B as are present in the total potential, but little is known about the higher coefficients.

4. Polarizable polar fluids

Assigning to each atom a permanent dipole moment $\boldsymbol{\mu}_0$ in addition to its fluctuating moment $\mathbf{p}$ introduces for each atom two new degrees of freedom, the Euler angles ω_0 for the direction of $\boldsymbol{\mu}_0$. The dipolar interactions now depend on the total moments $\mathbf{m}_j = \boldsymbol{\mu}_{0j} + \mathbf{p}_j$ of each particle j, with the fluctuating moments $\mathbf{p}_j$ again distributed according to the $f_0(p)$ of Eq. (24). However, the directions ω_0 can be immediately integrated out, so that we get a new distribution of just the relevant *total* moment m,

$$\begin{aligned} F_0(m) &\equiv \frac{1}{4\pi}\int d\omega_0 f_0(|\mathbf{m}-\boldsymbol{\mu}_0|) \\ &= \frac{\exp[-\beta\left(m^2+\mu_0^2\right)/2\alpha_0]}{(2\pi\alpha_0/\beta)^{3/2}}\,\frac{\sinh(\beta\mu_0 m/\alpha_0)}{\beta\mu_0 m/\alpha_0}. \end{aligned} \tag{37}$$

It is then clear that with the substitution $\mathbf{p}, f_0(p) \to \mathbf{m}, F_0(m)$, this is the *same calculation* as that of nonpolar polarizable molecules and can

TABLE 3. Computed thermodynamic and electrostatic properties of a polarizable polar LJ fluid for $\rho\sigma^3 = 0.80$ and $k_BT/\epsilon = 1.35$; MD data are from Pollock *et al.* [24]. The simulation uncertainties in the last digit of ε are given in parenthesis. $\mu^* \equiv \mu/(\epsilon\sigma^3)^{1/2}$.

μ_0^*	α_0/σ^3		$U/N\epsilon$	$\beta p/\rho$	ξ_2	ξ_4	μ^*	α/σ^3	ε
0.50	0	MD	-5.28				0.50		1.78(4)
		RHNC	-5.326	2.347	0	0	0.50	0	1.75
		HNC	-5.030	3.846	0	0	0.50	0	1.75
		SSC	-5.034	3.829	0	0	0.50	0	1.75
0.50	0.050	MD	-5.41				0.53		2.79(4)
		RHNC	-5.504	2.247	-0.195	0.001	0.528	0.0528	2.76
		HNC	-5.217	3.744	-0.203	0.001	0.529	0.0529	2.76
		SSC	-5.231	3.683	-0.205	0	0.530	0.0530	2.78
0.50	0.075	MD	-5.45				0.57		3.41(7)
		RHNC	-5.648	2.177	-0.307	0.002	0.554	0.0830	3.52
		HNC	-5.371	3.661	-0.323	0.003	0.556	0.0834	3.53
		SSC	-5.394	3.563	-0.326	0	0.557	0.0835	3.58
1.50	0	MD	-7.96				1.50		21(1)
		RHNC	-7.914	1.125	0	0	1.50	0	20.5
		HNC	-7.720	2.537	0	0	1.50	0	20.0
		SSC	-7.971	1.654	0	0	1.50	0	26.1
1.50	0.025	MD	-8.43				1.62		31(2)
		RHNC	-8.753	0.854	-2.790		1.612	0.0269	31.5
		HNC	-6.907	2.220	-2.923		1.617	0.0270	32.7
		SSC	-8.897	0.968	-2.920	0	1.617	0.0270	44.1

be solved with the same algorithm. Only the numerical coefficients in the polynomials $Q_{nl}(m)$ will be different. Since $F_0(m)$ with finite μ_0 is not a classical weight function, the $Q_{nl}(m)$ are constructed explicitly using Gram-Schmidt orthogonalization [13, 20]. For this one needs the moments $\langle m^{2j}\rangle$ of $F_0(m)$, which are readily calculated. As in the nonpolar case, it is found in practice [21] that the functional form of the distribution $F_0(m)$ remains essentially unchanged in a calculation, but the polarizability and permanent moment take on new effective values, $\alpha_0 \to \alpha$ and $\mu_0 \to \mu$.

The thermodynamic, dielectric, and structural properties of a system of polar polarizable LJ atoms have been calculated for a large number of states [21]. A sample of results is shown in Table 3 [22]. These calculations follow the same integral equation procedures described earlier, using three specific closures: optimized RHNC (again with hard-sphere bridge function), HNC, and single superchain (SSC) [23], also known as linearized-HNC. The simulation data used for comparisons are from Pollock *et al.* [24]. The three

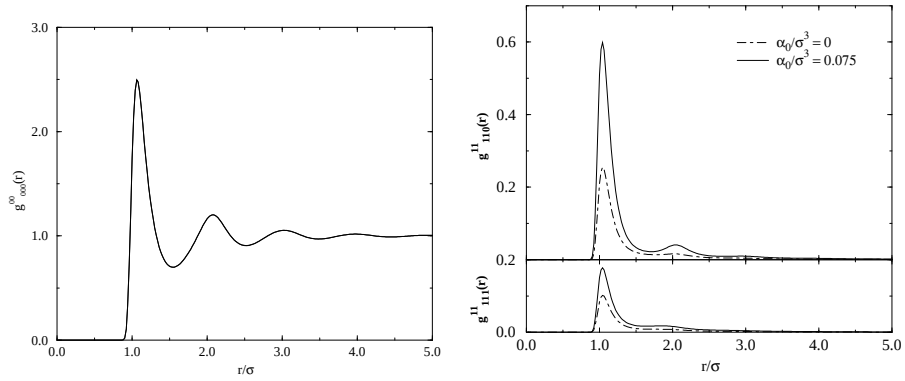

Figure 2. Distribution function coefficients of a polarizable polar Lennard-Jones liquid at density $\rho\sigma^3 = 0.80$ and temperature $k_BT/\epsilon = 1.35$. Computed results using the RHNC equation with permanent dipole moment $\mu_0 = 0.50(\epsilon\sigma^3)^{1/2}$ and two polarizabilities, $\alpha_0 = 0$ and $\alpha_0 = 0.075\sigma^3$. (a) *Left figure.* $g^{00}_{000}(r)$; the two curves are indistinguishable on this scale. (b) *Right figure.* $g^{11}_{110}(r)$ and $g^{11}_{111}(r)$.

closures give generally similar results. Where the disparities are greatest, the RHNC value gives the closest agreement with simulation.

For the smaller dipole moment in Table 3, the electrostatic effect of increasing the polarizability from 0 to $0.075\sigma^3$ is to double the dielectric constant ε. In Figs. 2(a) and 2(b), I show the corresponding structural effects. One sees that the geometrical packing of the atoms, reflected in the radial distribution functions of Fig. 2(a), is hardly affected by the increase in polarizability; the two curves are not distinguishable on this scale. However, the principal electrostatic coefficients of $g(\mathbf{r}_{12}, \mathbf{m}_1, \mathbf{m}_2)$ (which determine ε), shown in Fig. 2(b), are greatly increased in amplitude. This behavior agrees qualitatively with simulation findings [24] and is representative in general of the computed results.

It will be noted that, compared to earlier studies of fluids of polar nonpolarizable molecules [25], the cost of polarizabilty in the previous section was an additional two degrees of freedom in the pair functions and so two additional indices in the expansion coefficients, a manageable increase in numerical complexity. In this section, we find that extending the technique to polar polarizable molecules entails *no further increase in complexity.* The orthogonal polynomial method makes polar polarizable fluids as easy to study as nonpolar polarizable systems. In programming terms, one merely replaces the subroutine that calculates the orthogonal polynomials.

5. Charged particle in a polarizable fluid

The strength $E(r)$ of the electric field created by a point charge q immersed in a dielectric fluid is conventionally described as that of the charge in vacuum reduced by a constant factor ε, the dielectric constant of the medium:

$$\mathbf{E}(\mathbf{r}) = \frac{q}{\varepsilon r^2}\hat{\mathbf{r}}, \tag{38}$$

where $\hat{\mathbf{r}}$ is a unit vector in the radial direction $\mathbf{r}$. At the molecular level, this relation will still hold for r large, but for distances r out to a few atomic diameters from the particle with point charge q the Maxwell field $E(r)$ will reflect the local structure of the dielectric medium, so that ε is no longer constant. More generally, we may define a screening function $F(r)$ such that

$$E(r) = \frac{q}{r^2}\left[1 - F(r)\right]. \tag{39}$$

Then for large r we should expect $F(r) \sim (\varepsilon - 1)/\varepsilon$, while for small r the finite size of the charged particle should lead to $F(r) \approx 0$ inside its first near-neighbor shell, or core region. With the polarizable fluid modeled as in Section 3, it is possible to express $F(r)$ in terms of a *computable* pair distribution function coefficient [26].

The model consists of $N+1$ particles, labeled 0 through N, all of which interact pairwise with each other through a common LJ potential $u_0(r)$. Particle 0 carries a point charge q and its location defines the origin of coordinates. It is not polarizable. The remaining N particles are polarizable nonpolar molecules with molecular polarizability α_0. Their instantaneous point dipoles lead to additional interactions, through dipole-dipole forces with each other and through charge-dipole forces with particle 0. Thus the total potential energy of an instantaneous configuration of positions $\mathbf{r}_j$ and dipole moments $\mathbf{p}_j$ is

$$\mathcal{U} = \sum_{0\le i<j\le N} u_0(r_{ij}) + \sum_{1\le i<j\le N} u_{dd}(\mathbf{r}_{ij}, \mathbf{p}_i, \mathbf{p}_j) + \sum_{1\le j\le N} u_{cd}(\mathbf{r}_{0j}, \mathbf{p}_j), \tag{40}$$

where $u_{cd}(\mathbf{r}, \mathbf{p}) = -q(\hat{\mathbf{r}} \cdot \mathbf{p})/r^2$.

With the contribution of the dipoles added to the central field made by charge q at the origin, the mean electric field at position $\mathbf{r}$ is

$$\mathbf{E}(\mathbf{r}) = \frac{q}{r^2}\hat{\mathbf{r}} + \int d\mathbf{r}' d\mathbf{p}' \frac{\rho f(p') g(\mathbf{r}', \mathbf{p}')}{|\mathbf{r} - \mathbf{r}'|^3}\left[3\frac{\mathbf{p}' \cdot (\mathbf{r} - \mathbf{r}')}{|\mathbf{r} - \mathbf{r}'|^2}(\mathbf{r} - \mathbf{r}') - \mathbf{p}'\right], \tag{41}$$

where $g(\mathbf{r}, \mathbf{p})$ is the pair distribution function of particle 0 with the polarizable molecules of instantaneous polarization $\mathbf{p}$. To evaluate the integrals

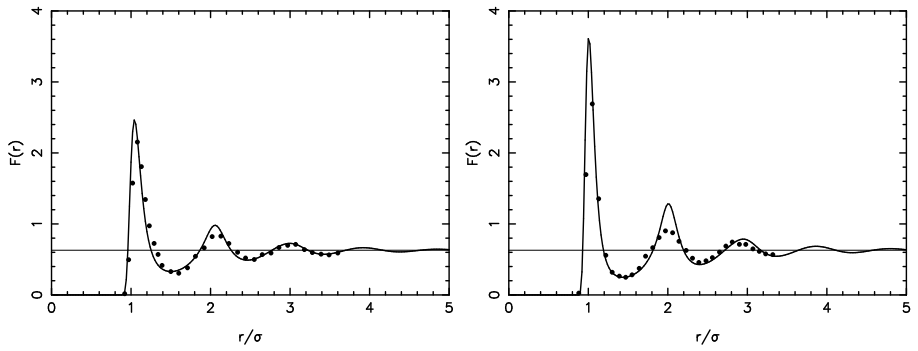

Figure 3. Screening functions $F(r)$ for a charge q in a liquid of polarizable nonpolar molecules: solid lines – HNC; points – MD [28]. The light horizontal lines are the asymptotic limit $(\varepsilon - 1)/\varepsilon = 0.63$. (a) *Left figure.* $q = 0.01(\epsilon\sigma)^{1/2}$. (b) *Right figure.* $q = 10(\epsilon\sigma)^{1/2}$.

in Eq. (41), we make use of the polynomial basis sets of Section 3 to break out the $\mathbf{p}$ dependence in $g(\mathbf{r}, \mathbf{p})$,

$$g(\mathbf{r}, \mathbf{p}) = (4\pi)^{1/2} \sum_{n,l} g_l^n(r) Q_{nl}(p) Y_{l0}(\omega). \tag{42}$$

The integrations can now be done explicitly; it is straightforward to show that the total radial field becomes simply [26]

$$E(r) = \frac{q}{r^2} - \left(\frac{\alpha}{\beta}\right)^{1/2} 4\pi\rho g_1^1(r) \tag{43}$$

and so the screening function is $F(r) = 4\pi\rho\alpha r^2 g_1^1(r)/q(\alpha\beta)^{1/2}$.

The system composed of charge q immersed in a fluid of N polarizable molecules constitutes a two-component mixture with one component at infinite dilution. We can thus adapt the usual equations for liquid state mixtures [1] to calculate the charge-dipole and dipole-dipole distribution functions, $g(\mathbf{r}_{01}, \mathbf{p}_1)$ and $g(\mathbf{r}_{12}, \mathbf{p}_1, \mathbf{p}_2)$, respectively. The latter calculation was described in Section 3; $g(\mathbf{r}_{01}, \mathbf{p}_1)$ is found by a similar, but simpler, procedure which incidently ensures the correct asymptotic limit, $F(r) \sim (\varepsilon - 1)/\varepsilon$ [26].

The only available simulation data for a model of a charged particle in a polarizable nonpolar fluid appear to be those of Pollock and Alder [27, 28] for a liquid state of Lennard-Jones molecules near the triple point: $\rho\sigma^3 = 0.844$, $k_BT/\epsilon = 0.85$, $\alpha_0/\sigma^3 = 0.10$. Thus, the results given here are for this same state. (The computed values of α and ε for this state are $\alpha/\sigma^3 = 0.1115$ and $\varepsilon = 2.699$.)

Figures 3(a) and 3(b) show the screening functions $F(r)$ obtained using the HNC equation for two different charges, $q/(\epsilon\sigma)^{1/2} = 0.01$ and 10. The second of these corresponds to about half an elementary charge, $q \approx 0.5e$, if argon values are used for the LJ parameters: $\sigma = 3.4$ Å and $\epsilon = 120k_B$, so $e/(\epsilon\sigma)^{1/2} = 20.2$. The figures are drawn to the same scale so the effect of increasing the charge q is more readily apparent. Comparison of the HNC results with the simulation data shows reasonably good agreement.

References

1. J. P. Hansen and I. R. McDonald, *Theory of Simple Liquids* (Academic, London, 1986).
2. M. S. Green, J. Chem. Phys. **43**, 1403 (1960). The parallel set $P(r)$ of this paper is not the same as that of Eq. (1).
3. J. K. Percus and G. J. Yevick, Phys. Rev. **110**, 1 (1958).
4. C. G. Gray and K. E. Gubbins, *Theory of Molecular Fluids* (Clarendon, Oxford, 1984), Vol. 1.
5. F. Lado, Phys. Rev. E **54**, 4411 (1996).
6. B. D'Aguanno and R. Klein, Phys. Rev. A **46**, 7652 (1992) and private communication.
7. F. J. Rogers and D. A. Young, Phys. Rev. **30**A, 999 (1984).
8. F. Lado, J. Chem. Phys. **108**, 6441 (1998).
9. J. C. Crocker and D. G. Grier, Phys. Rev. Lett. **73**, 352 (1994).
10. J. S. Høye and G. Stell, J. Chem. Phys. **73**, 461 (1980).
11. L. R. Pratt, Mol. Phys. **40**, 347 (1980).
12. F. Lado, Phys. Rev. E **55**, 426 (1997).
13. See, for example, G. Arfken, *Mathematical Methods for Physicists* (Academic, Orlando, 1985), Chap. 9.
14. P. M. Morse and H. Feshbach, *Methods of Theoretical Physics* (McGraw-Hill, New York, 1953), p. 1662ff.
15. F. Lado, Mol. Phys. **47**, 283 (1982).
16. E. L. Pollock and B. J. Alder, Phys. Rev. Lett. **39**, 299 (1977).
17. F. Lado, Phys. Rev. A **8**, 2548 (1973).
18. Y. Rosenfeld and N. W. Ashcroft, Phys. Rev. A **20**, 1208 (1979).
19. F. Lado, Phys. Lett. **89A**, 196 (1982).
20. N. I. Akhiezer, *The Classical Moment Problem* (Hafner, New York, 1965), Chap. 1.
21. F. Lado, E. Lomba, and M. Lombardero, J. Chem. Phys. **108**, 4530 (1998).
22. The computed results for $\alpha_0 = 0$ in Table 3 are obtained using the simpler algorithm for nonpolarizable dipolar systems described some time ago [25]. They are included here for completeness.
23. M. S. Wertheim, Mol. Phys. **26**, 1425 (1973).
24. E. L. Pollock, B. J. Alder, and G. N. Patey, Physica **108A**, 14 (1981).
25. F. Lado, M. Lombardero, E. Enciso, S. Lago, and J. L. F. Abascal, J. Chem. Phys. **85**, 2916 (1986).
26. F. Lado, J. Chem. Phys. **106**, 4707 (1997).
27. E. L. Pollock and B. J. Alder, Phys. Rev. Lett. **41**, 903 (1978).
28. E. L. Pollock, B. J. Alder, and L. R. Pratt, Proc. Natl. Acad. Sci. USA **77**, 49 (1980).